

Hannu Holma, Antti-Jussi Mattila, Aappo Roos, Timo Hyvärinen, and Oliver Weatherbee
Specim, Spectral Imaging Ltd., POB 110, FIN-90591 Oulu, Finland
SpecTIR LLC, 11781 Lee Jackson Memorial Highway, Suite 210, Fairfax, VA 22033, USA

Keywords: Hyperspectral imaging, hyperspectral sensor, LWIR, infrared, thermal, spectral camera, pushbroom, airborne, chemical imaging, mineral mapping, mineral identification, UAV, sorting

"Thermal hyperspectral imaging in the LWIR"

Hyperspectral imaging systems have recently gained importance in biomedical, chemical and industrial applications. Nevertheless in high-end sectors, such as aerospace and defense, hyperspectral imaging technology is constantly developed towards new capabilities. Year 2011, Specim introduced the LWIR-C, world's first UAV ready thermal infrared hyperspectral camera.⁷ In this article we see how this ultimate performance camera compares to the second generation version of its predecessor, Specim LWIR-HS, a moderate priced thermal infrared spectral camera designated for industrial applications. Both imagers employ an imaging spectrograph with a transmission grating and on-axis optics.

The compact size yet superior performance of the presented LWIR instruments is a rare and remarkable combination in hyperspectral thermal imaging. In the past liquid nitrogen cooled optics has been a prerequisite to control the instrument radiation, leading to bulky and complicated systems. Instrument radiation is a much bigger challenge in a hyperspectral instrument than in a broadband camera because the optical signal from the target is spread spectrally, but the instrument radiation is not dispersed. Without any suppression, the instrument radiation can overwhelm the radiation from the target even by 1000 times. Only through novel inventions it is possible to control the instrument radiation – resulting in LWIR-C 's signal-to-noise ratio, SNR better than 700 at 10 μm wavelength for a 300 K target optical path being in ambient temperature.

The detector type largely determines the performance of the thermal hyperspectral camera, and the applications where it can be used. This paper presents practical measurements of the compact LWIR-C and LWIR-HS hyperspectral cameras. The LWIR-C hyperspectral camera utilizes a Mercury Cadmium Telluride, MCT sensor coupled with a stirling-cycle cooler, whereas the moderately priced LWIR-HS utilizes an uncooled microbolometer FPA.

1 INTRODUCTION

Hyperspectral imaging in the long wave infrared (LWIR, 7 to 14 μm) region is gaining increasing interest. There are very few instruments available which can provide both good performance and usability. SEBASS instrument is still a reference imager in LWIR airborne experiments, but it requires special expertise in its operation and maintenance.^{1, 2} With the increasing defense and commercial interest in thermal spectral imaging, instrument suppliers are developing both push-broom and Fourier Transform (FT) imaging spectrometers for field, laboratory and airborne measurements.³

Year 2011 Specim introduces two new LWIR hyperspectral imagers: the new high-performance LWIR-C thermal camera and the second generation of its predecessor LWIR-HS. High sensitivity and stability, compact size, and low maintenance have been the driving design targets for these cameras.

The main LWIR-HS improvement is the enhanced microbolometer detector. The LWIR-C camera encompasses the most advanced custom made MCT detector array, providing outstanding sensitivity across the broad spectral range of 7.7 to 12.4 μm with low dark current and high pixel well capacity. The detector applied is at minimum 10 times more sensitive than any existing microbolometer array. The first experimental data of these two novel cameras are presented and compared in this paper.

2 OVERVIEW OF THE LWIR SPECTRAL IMAGERS

The LWIR imagers presented here are push-broom type hyperspectral imagers. A push-broom imager is the only hyperspectral technology that can be used for laboratory, field, and on-line measurements.

The LWIR-HS hyperspectral camera is ideal for industrial applications where the measured targets either have high temperature (emission measurement) or can be illuminated with a high temperature radiation source (reflectance measurement). LWIR-HS' numerical aperture is matched to that of the microbolometer detector (F/1.0) in order to maximize the light collection efficiency and sensitivity of the camera. Unlike in the LWIR-C, the spectrograph of the LWIR-HS is designed to provide broader spectral band per pixel *id est* lower resolution in order to collect more energy per pixel. The camera structure is extremely compact and power consumption low, as presented in Table 1.

The LWIR-C camera, provides the highest performance in terms of spectral resolution, sensitivity and signal-to-noise ratio, which are needed for the demanding airborne and defense applications. A typical airborne application is

mineral mapping for geological exploration. Defense and law enforcement applications, such as target recognition, benefit from the fact that no external light source such as the sun or moon is needed for chemical mapping. Without compromising performance, the LWIR-C measures 285x200x175 mm and weights 13.5 kg only, being compact enough for mini-size Unmanned Aerial Vehicles, UAVs.

Table 1 summarizes the main specifications of the LWIR-C and LWIR-HS spectral cameras, as seen in Figure 1. Results from the performance evaluation of the cameras are presented in chapters 4,5, and 6.

Table 1. The main specifications of the LWIR-C and LWIR-HS spectral cameras. The LWIR-C data applies to the AisaOWL airborne remote sensing system sensor.

	LWIR-C	LWIR-HS
F#	2.0	1.0
Wavelength range	8.0 – 12.0 μm	7.8 – 12.0 (13.0)
Number of spectral pixels	84	30 (42)
Number of spatial pixels	384	384
Spectral resolution	100 nm	400 nm
Detector type	MCT	Microbolometer
Spectral sampling	48 nm	200 nm (mean)
Instrument temperature	300 K	300 K
Instrument temperature control	Stabilized	None
Camera dimensions	175x285x200 (mm)	55x130x125 (mm)
Camera weight	13 kg	3.5 kg
Power consumption	200 W	3.5 W



Figure 1. The micropolometer spectral camera Specim LWIR-HS (left), and MCT spectral camera Specim LWIR-C (right).

3 CALIBRATION PROCEDURES

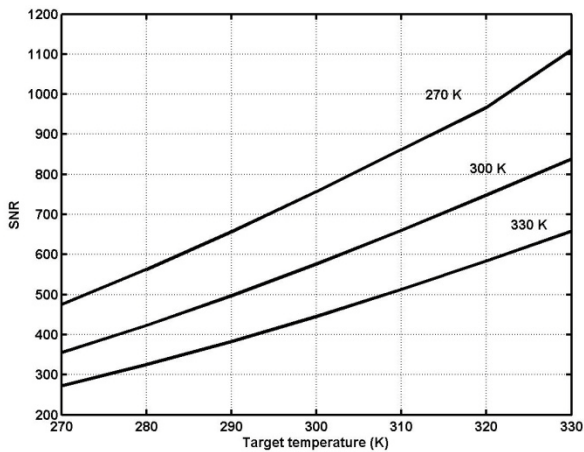
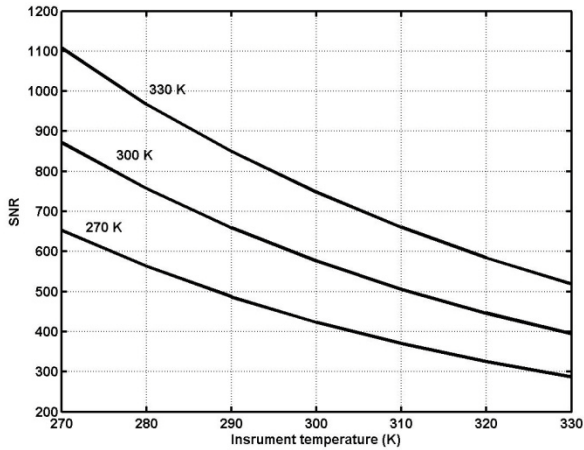
The two main calibration actions are needed for a hyperspectral imager: spectral and radiometric calibration. These basic calibrations are needed to match the wavelength and spectral radiance of the target with the band and signal of the imaging instrument.

The signal of the imager correlates with the spectral radiance of the target, but it also correlates with the instrument radiation depending on the instrument temperature. Specim's unique approach, applied in the LWIR-C, has been to develop an instrument and a calibration system that does not need any external blackbody calibrators carried with the instrument. This is achieved through several inventions in the instrument design and background monitoring on chip, BMC. For example, the instrument radiation is being measured continuously, and the actual background signal is subtracted from each frame. The novel BMC method offers several advantages in comparison to the commonly used method of doing blackbody calibrations only before and after the measurement sequences.

4 PERFORMANCE TEST RESULTS OF THE SPECIM LWIR-C

The amount of the instrument radiation depends on the instrument temperature. Consequently, the sensitivity and the SNR of the camera depend on the set operation temperature of optics. Figure 2 shows how the SNR in the LWIR-C spectral camera varies with the set instrument optics temperature, and how it also depends on the target temperature. The results are obtained from a spectral camera simulation model which takes into account the detailed properties of the fore lens, imaging spectrometer, detector array, instrument radiation, and target. It has been verified experimentally that the model simulates the spectral camera performance very accurately.

The most common performance parameter with thermal IR cameras is traditionally NETD (noise equivalent temperature difference). However, this figure of merit is not well applicable to spectral instruments, because it also depends on the temperature, and spectral emissivity of the target. The most descriptive figure of merit for a thermal hyperspectral camera is NESR (noise equivalent spectral radiance). It does not depend on the target properties, but is unique to the instrument, and allows immediate estimation of the SNR once the spectral radiance of the target is known. ^{4, 5}



a)

b)

Figure 2. The SNR in the LWIR-C camera at 10 μm wavelength as a function of the set instrument optics temperature, with a blackbody target at three temperatures, 270 K, 300 K and 330 K (left). The diagram on the right shows the SNR as a function of a blackbody target temperature with the instrument set to three different temperatures.

For the radiometric calibration and experimental determination of the NESR and SNR, a series of measurements with a precisely calibrated blackbody radiator were performed. A series of 1000 images was taken from the blackbody at five different temperatures from 10 °C to 50 °C with 10 °C intervals.

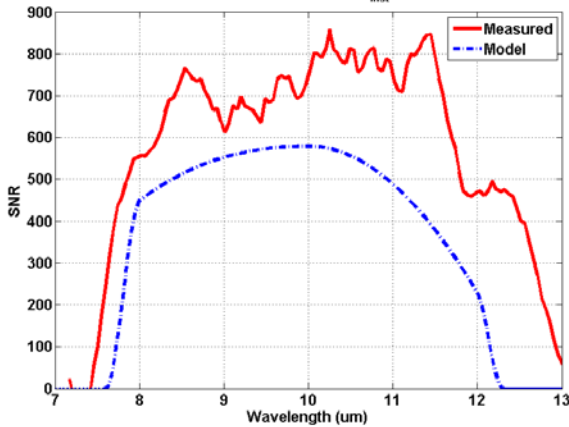
NESR and SNR were calculated for each pixel from the measured data. The temporal noise of a pixel is determined as the standard deviation of the signal in the 1000 frames. The SNR is calculated as the ratio of the target signal to noise. The spectral SNR, with the peak signal filling 90% of the well capacity is shown in Figure 3 together with the simulated SNR values. The measured SNR exceeds the

simulation which is mainly due to higher signal than originally expected. The SNR is excellent over a broad spectral region from 7.7 μm to 12.4 μm .

NESR is determined as the ratio of noise to radiance sensitivity. Figure 3 shows the NESR at the middle of the field of view when the instrument optics temperature is set to +22 C. The NESR is at the level of 15 $\text{mW}/(\text{m}^2 \cdot \text{sr} \cdot \mu\text{m})$ from 8 μm to 11.5 μm and below 25 $\text{mW}/(\text{m}^2 \cdot \text{sr} \cdot \mu\text{m})$ through the whole design wavelength range of 8 μm to 12 μm . The measured NESR follows very well the simulation results as shown in Figure 3. Also NETD was calculated also for the LWIR-C spectral camera, and it is at the level of 0.2 K for the most of the design spectral range of 8 μm to 12 μm .

The measured figures of merit for the spectral camera LWIR-C are summarized in Table 2 at 8 μm , 10 μm , and 12 μm . The Specim LWIR-C spectral camera is also used as the imager in an airborne thermal hyperspectral system AisaOWL, and thus the same performance figures apply to the airborne system.

Modelled and measured SNR; averaged by two pix; $T_{\text{inst}} = 22\text{C}$, 30.03.2011, tint = 2.1ms



Modelled and measured NESR; averaged by two pix; $T_{\text{inst}} = 22\text{C}$, 30.03.2011, tint = 2.1ms

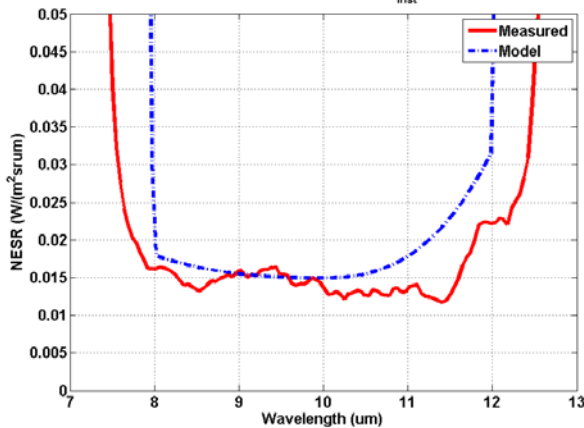


Figure 3. SNR (left) and NESR (right) in the spectral camera LWIR-C at the middle of the field of view as a function of wavelength (left). Both simulated and measured curves are shown. The data has been averaged by two spectral pixels.

Table 2. The measured figures of merit of the LWIR-C spectral camera apply also to the AisaOWL airborne hyperspectral system. Instrument optics temperature is 22 °C and target is a blackbody at 30 °C temperature.

	SNR	NESR (mW/m ² srμm)	NETD (K)
8 μm	557	16.2	0.13
10 μm	758	13.6	0.11
12 μm	468	22.2	0.25

5 PERFORMANCE TESTS OF THE SPECIM LWIR-HS

The LWIR-HS spectral camera and its performance figures were for the first time presented in SPIE DSS conference in 2009⁶. The second generation LWIR-HS has the latest state-of-the-art microbolometer detector: the sensitivity has improved by a factor of 3 and the SNR is about 15% higher. The experimental arrangement is the same as in the original measurements. The signal for each of the target blackbody temperatures and SNR are presented in Figure 4.

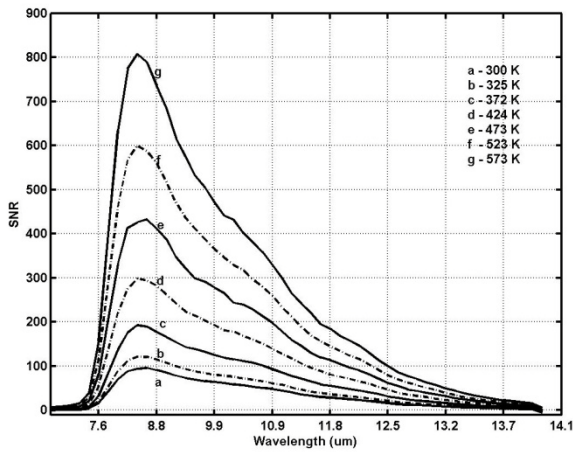
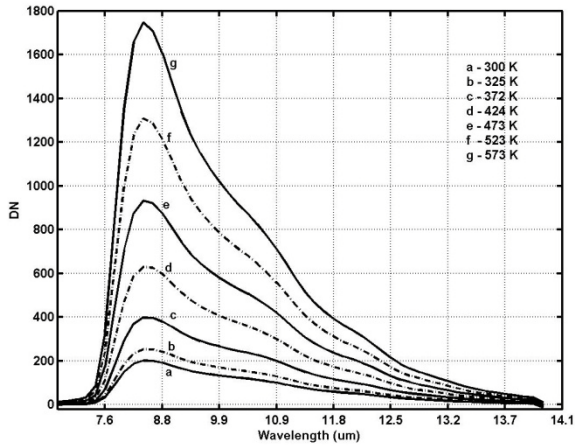


Figure 4. Signal (left) and SNR (right) of the second generation LWIR-HS camera with different blackbody target temperatures. Zero signal level refers to 0 K target.

Table 3 summarizes the SNR with different target temperatures. The data quality can be improved by averaging up to three pixels in spectral direction without degrading spectral resolution significantly. The mean spectral resolution is 400 nm whereas the spectral sampling in the new version is 145 nm.

Table 3. SNR of the second generation LWIR-HS camera at 8 μm with a blackbody target at different temperatures. Data is for one pixel and no averaging or binning is performed.

Target temperature (K)	SNR
296	41
323	70
473	150
423	265

473	420
523	620
573	840

6 GUIDELINES FOR THE LWIR-HS AND LWIR-C USAGE

Some guidelines for usage of the LWIR-HS and the LWIR-C are presented in the Table 4. The performance of the LWIR-C is superior, but for some applications a moderate cost microbolometer based system may be more attractive.

The performance of the scanning imager may be improved by employing a lower scan speed to enable averaging of successive frames in data processing. Also binning spectral bands may be applied to improve the SNR. This is applicable if lower spectral resolution is acceptable. These compromises enhance the SNR of the LWIR-HS but are not needed for the LWIR-C camera.

Table 4. Comparison of the performances of LWIR-C and LWIR-HS in terms of SNR and NESR. The LWIR-C data applies also to the AisaOWL airborne hyperspectral system.

300 K target	LWIR-C	LWIR-HS	LWIR-HS 'slow scan' x10	LWIR-HS '4-band binning'
NESR@10um [mW/m ² sr μm]	20	160	50	60
SNR@10um	580	~35	110	95
Imager cost (relative)	1	0.1	0.1	0.1

7 APPLICATION EXPERIMENTS

Laboratory and industrial chemical LWIR-C and LWIR-HS imaging experiments in reflection mode

The LWIR-HS and LWIR-C are the first commercially available hyperspectral imagers enabling thermal infrared based chemical imaging for industrial applications. Until now industrial hyperspectral chemical imaging has been limited to visible/near infrared, VNIR and short-wave infrared, SWIR spectral ranges.

However, several target materials have their most distinctive and strongest spectral signature in the LWIR regions. For example, geological samples, like drill cores, can be rapidly mapped for nearly all minerals of commercial interest with the fusion of SWIR and LWIR spectral imaging. LWIR is practically mandatory for the detection of minerals in feldspar, silica, calcite, garnet, and olivine groups.

Figure 5 shows section of a drill core sample imaged by Specim VNIR, SWIR and LWIR-HS spectral cameras. The image was acquired in reflectance mode in each spectral region. Halogen lamps were used as a light source for the VNIR and SWIR cameras, whereas a quartz heater rod was used as an illumination source for the LWIR camera. Reliable mineral identification was achieved even though the LWIR illumination source was a prototype. The LWIR-HS data provides valuable supplementary information of the mineralogy, leading to reliable mineral identification.

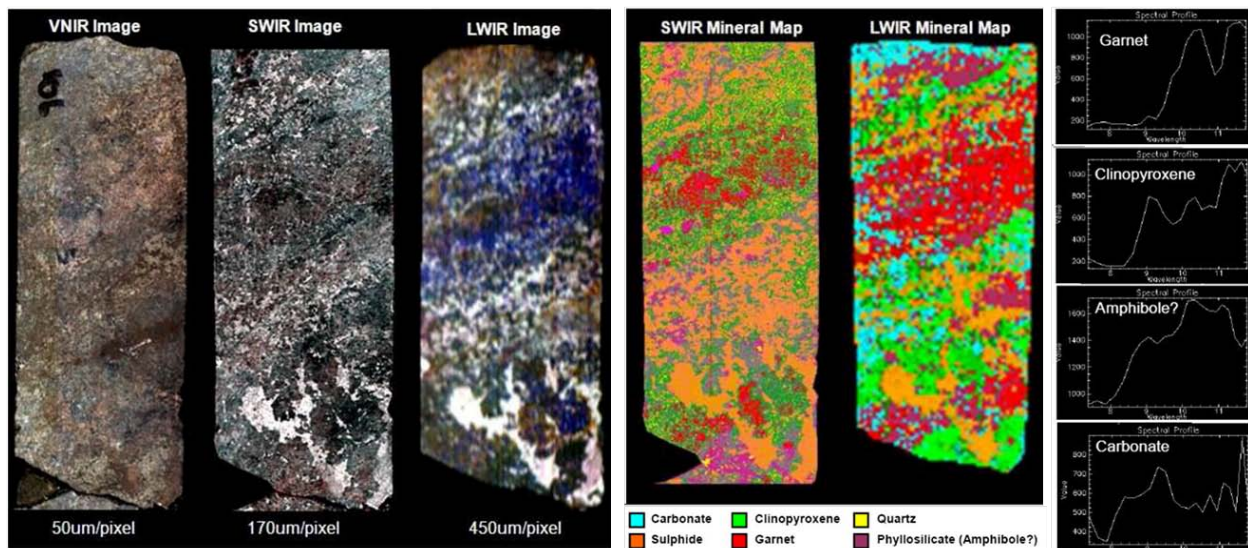


Figure 5. Reflectance measurement. Drill core samples measured with Specim VNIR, SWIR, and LWIR-HS cameras. An LWIR camera is mandatory for quartz, garnet, and feldspar mapping. Courtesy of AngloGold Ashanti.

Figure 6 presents a comparison of LWIR-HS and LWIR-C reflectance data in mineral identification. A quartz heater rod was used as an illumination source; the same measurement setup and spatial resolution was applied to both cameras. LWIR-C provides considerably better spectral sampling, spectral resolution, and dynamics throughout the full spectral range from 7.7 μm to 12.4 μm , leading to much more detailed spectral structure. Consequently, feldspar and quartz can easily be

distinguished from each other. Based on preliminary studies, the LWIR-C may even be able to separate plagioclase feldspars based on composition. This would have significant value in planning and optimizing commercial mining operations.

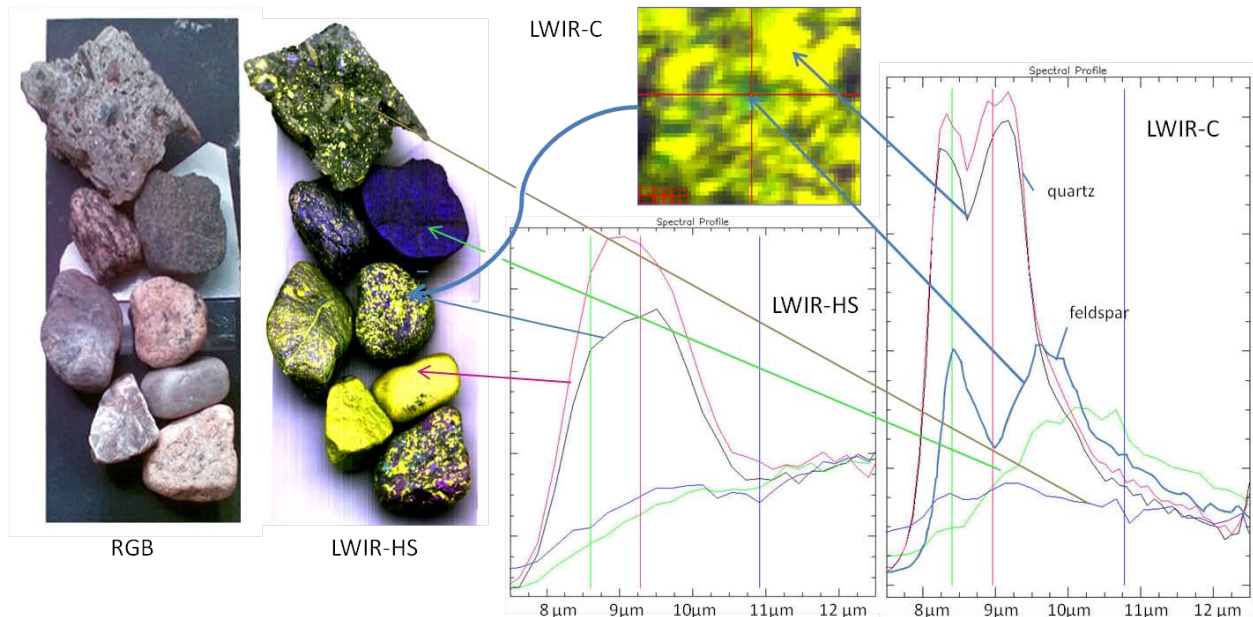


Figure 6. Reflectance measurement. A set of stones were scanned with LWIR-HS and LWIR-C imagers. The LWIR-C produces better sampling and resolution leading to much more accurate mineral identification. In the zoomed LWIR-C image the feldspar spectrum is clearly recognizable. The LWIR-C provides remarkably better response especially in the spectral region from 10.5 μm to 12.4 μm.

LWIR-C and LWIR-HS outdoor ground scan experiments

The LWIR-C hyperspectral camera provides the performance required for outdoor emission measurements, whereas the LWIR-HS camera usage for ambient temperature targets is rather limited. Still LWIR-HS' outdoor operation was demonstrated to provide comparison to LWIR-C data. Figures 8 and 9 show ad-hoc outdoor scans performed with the LWIR-HS and LWIR-C cameras.

The image in Figure 8 is scanned with first generation LWIR-HS imager. The second generation LWIR-HS would provide some improvements in spectral data as described in the paragraph 5, but the image would be visually comparable. The LWIR data has been normalized using 60°C and 3°C blackbody targets as normalization references: $\text{normalized data} = (\text{data} - \text{cold reference}) / (\text{warm reference} - \text{cold reference})$. The LWIR-HS image shows several visible details: The frame of the windows has a slight temperature difference to the window blinds and

to the wall. A hot fan can be seen as a bright spot on a tripod, the black rectangle below is an ordinary paper booklet. Even if the LWIR-HS has been designed for reflectance measurements with artificial illumination, it may be applied to emission measurements in some research applications.

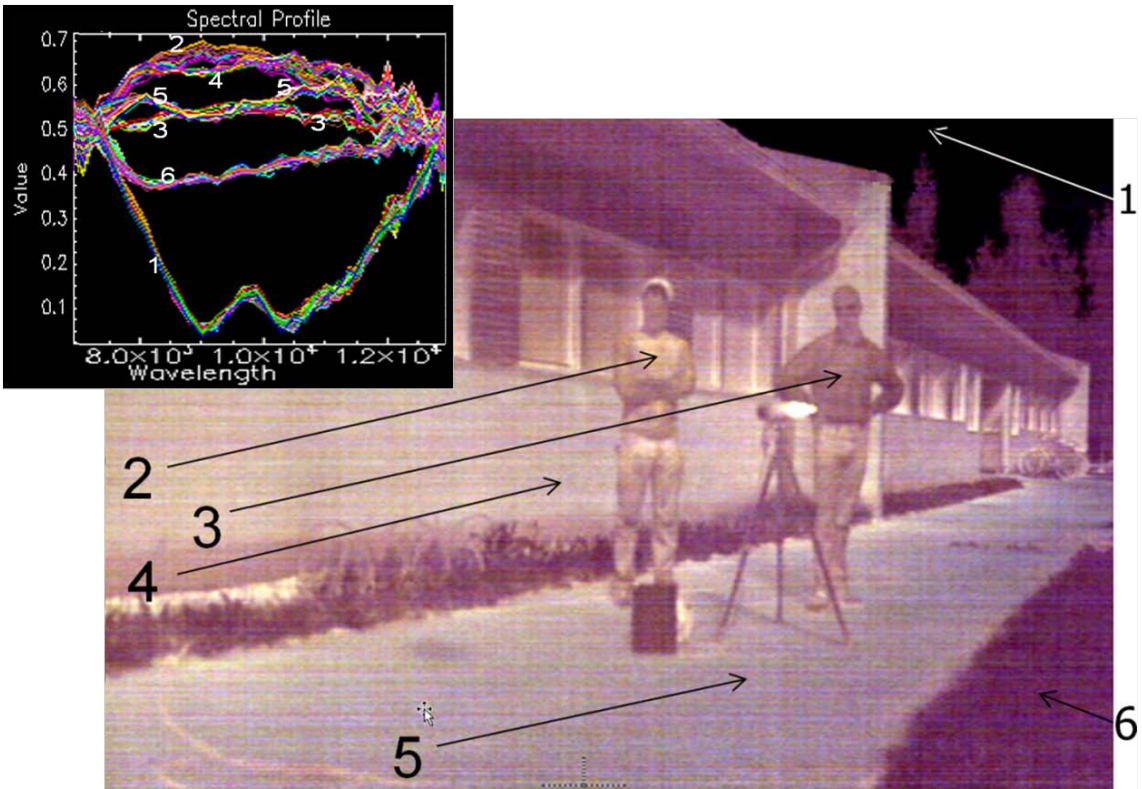


Figure 8. Emission measurement. An outdoor scan experiment (August, 2010) with the LWIR-HS camera, ambient temperature well above +10°C. Relative spectra from various targets in the image are shown: 1. Sky with ozone emission, 2. Shirt of person one, 3. Shirt of person two, 4. Brick wall, 5. Pavement, 6. Grass.

Figure 9 shows an LWIR-C outdoor scan in winter conditions (-15°C). Despite the significant temperature difference of close to 30K, the LWIR-C data is superior in comparison to the LWIR-HS measurement (Figure 8). The spectra of the different objects have clearly distinctive characteristics. For example, the characteristic emission spectrum of watch glass visible in Figure 9 would not be identifiable with the LWIR-HS. Radiometric correction was applied to LWIR-C data.

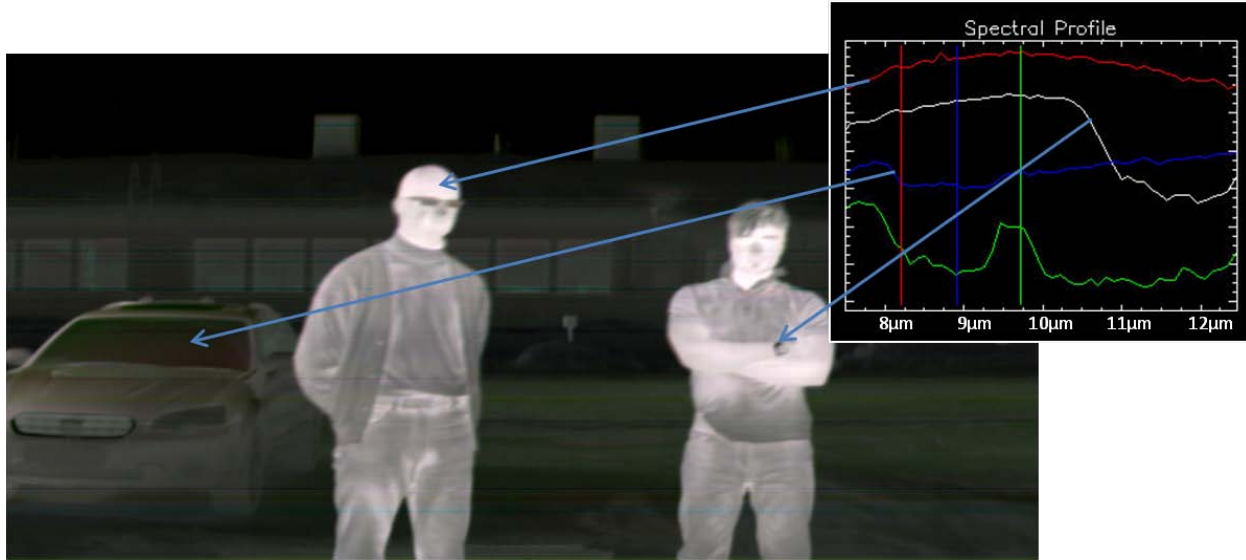


Figure 9. Emission measurement, an outdoor scan experiment with the LWIR-C camera in winter conditions (February 2011), ambient temperature -15°C . Relative spectra from various targets in the image are shown with arrows. The green spectrum shows clear sky, the emission from ozone layer is clearly visible.

LWIR-C Flight experiment

A thermal airborne hyperspectral imaging system, AisaOWL, has been built using the LWIR-C hyperspectral camera. The first test flights were carried out with the system by SpecTIR LLC in March 2011. Data was collected with 1 m ground pixel size over the Reno city and Cuprite area in Nevada, USA. The city area was imaged to verify the camera's image quality and to calibrate the camera and GPS/INS sensor to each other for precise georeferencing. Figure 10 shows a flight line over downtown Reno. The gray levels in the figure represent the radiance level of the LWIR wavelength band. Data was collected in daylight conditions; there is a contribution of heating and reflection of sunlight in the measurement. Spectra from various targets show both spectral emissivity and temperature differences. The weather was sunny but cold, temperature just above 0°C , after a night subfreezing temperatures. There is some snow on the streets and roofs.

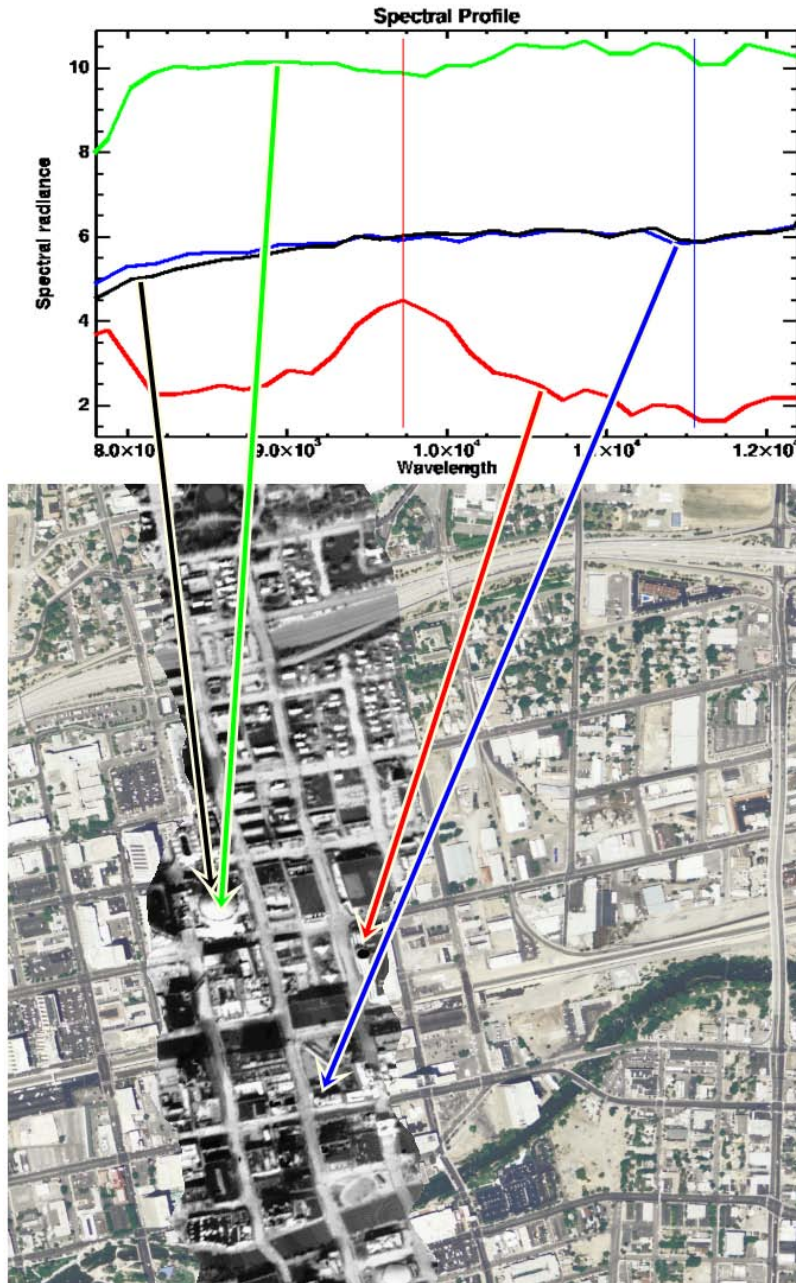


Figure 10. Emission measurement. An AisaOWL flight line over the downtown Reno, NV, USA at Feb 27 2011. The AisaOWL data is shown as black and white stripe in the middle of the image. It is embedded to visible range image to show compatibility. Blue curve is from a shadowy yard of a building. Red curve comes from circular very cold construction near Silver Legacy casino. Green and black curves are the spectra of the sunny and shadowy side of the dome of Silver Legacy casino respectively. Wavelength is in nanometers and spectral radiance in $W/(m^2 \cdot sr \cdot \mu m)$.

The Cuprite area in Nevada is one of the most extensively referenced areas for mineral mapping in the world. It has been imaged with several LWIR imagers, such as SEBASS, and thus it is a good reference area for acquiring mineral mapping data for evaluation of a new hyperspectral instrument. The flight line image in Figure 11 is georeferenced and mapped using a digital elevation model, ground resolution is 1 m. The weather was sunny and temperature just above 0° C, after a night subfreezing temperatures. There is no visible snow on the ground. Some examples of spectral shapes are shown in the Figure 11. Preliminary comparison show excellent correlation with available reference data. Detailed data analysis of this newly acquired data is ongoing (April 2011), the results will be published later.

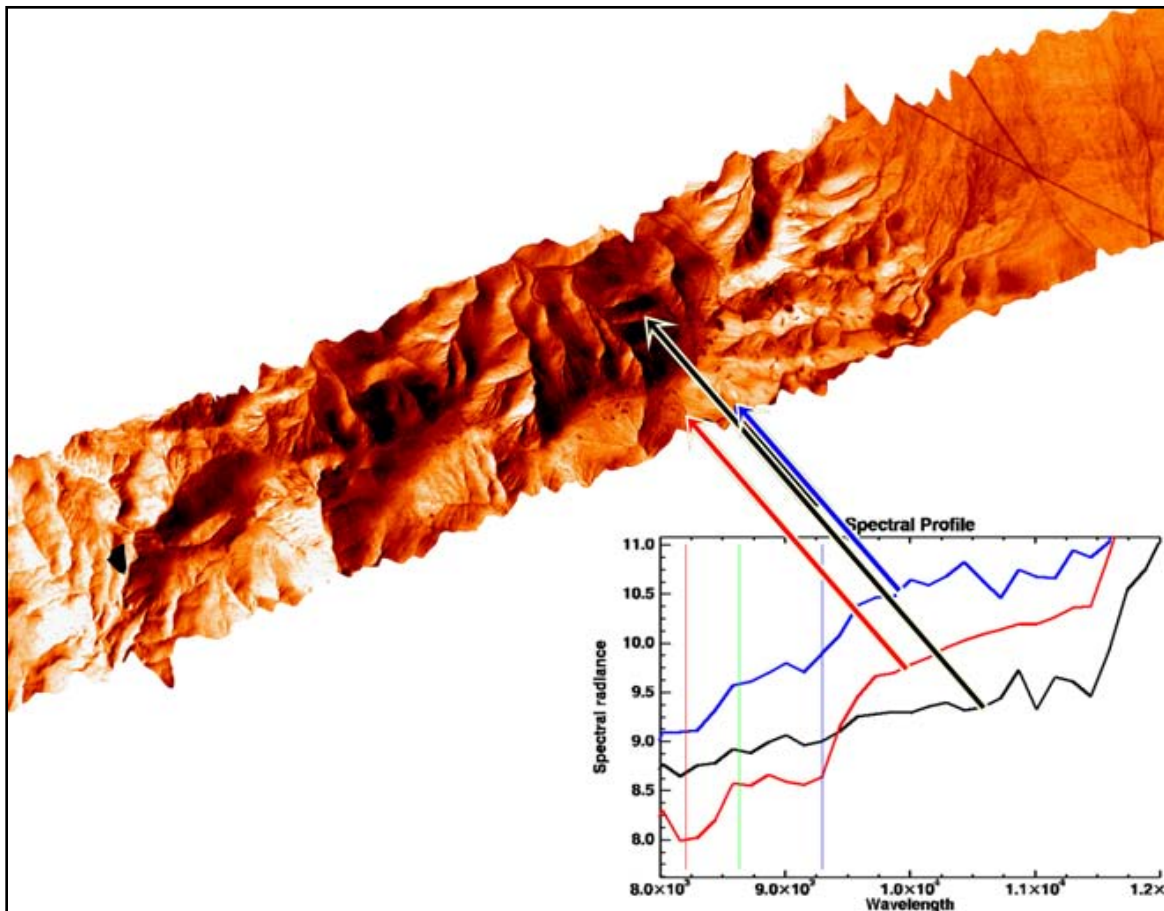


Figure 11. Emission measurement. Image of two adjacent AisaOWL flight lines over the Cuprite area, NV, USA flown on Feb 27 2011. Example spectra are shown in the graph with arrows pointing positions of samples. Wavelength is in nanometers and spectral radiance in $W/(m^2 \cdot sr \cdot \mu m)$.

8 CONCLUSIONS

The two new push-broom type hyperspectral imagers presented will make LWIR spectral imaging much more feasible in several application areas. The LWIR-C imager based on a deeply cooled MCT FPA is the first high sensitivity spectral imager which covers the total LWIR region from 7.7 to 12.4 μm , and is compact enough for installation even in UAVs, and is easy to operate in the field. The LWIR-C imager brings extra value to industrial, scientific, and defense applications where the high spectral resolution and best available signal-to-noise-ratio are crucial. The microbolometer based rugged LWIR-HS imager provides sufficient performance for LWIR chemical imaging in laboratory and industry at affordable cost.

REFERENCES

- [1] Kirkland, L. E., K. C. Herr, E. R. Keim, P. M. Adams, J. W. Salisbury, J. A. Hackwell, A. Treiman, First Use of an Airborne Thermal Infrared Hyperspectral Scanner for Compositional Mapping, *Remote Sens. Environ.* 80, 447–459, (2002).
- [2] Mares, A.G., Olsen, R.C., and Lucey, P.G., LWIR Spectral measurements of volcanic sulfur dioxide plumes, Proceedings of the SPIE, Volume 5425, pp. 266-272 (2004).
- [3] Chamberland, M., Belzile, C., Farley, V., Legault, J-F., and Schwantes, K., Advancements in field-portable imaging radiometric spectrometer technology for chemical detection, Proc. SPIE, Vol. 5416, 63 (2004).
- [4] Dereniak, E.L. and Boreman, G.D., Infrared Detectors and Systems, John Wiley & Sons, (1996).
- [5] Kruse, P.W., Uncooled Thermal Imaging, SPIE Tutorial Texts in Optical Engineering Vol. TT51, (2001).
- [6] Holma, H, T. Hyvärinen, J. Lehtomaa, H. Karjalainen and R. Jaskari, Proc. SPIE, Vol. 7319, 731907 (2009); DOI: 10.1117/12.818557.
- [7] World First Thermal Hyperspectral Camera for Unmanned Aerial Vehicles. Frost&Sullivan, Aerospace and Defense Technology Insight February 2011.